

MAPT Genetic Variation and Neuronal Maturity Alter Isoform Expression Affecting Axonal Transport in iPSC-Derived Dopamine Neurons

Joel E. Beevers,¹ Mang Ching Lai,¹ Emma Collins,¹ Heather D.E. Booth,¹ Federico Zamboni,¹ Laura Parkkinen,^{2,3} Jane Vowles,^{3,4} Sally A. Cowley,^{3,4} Richard Wade-Martins,^{1,3,*} and Tara M. Caffrey^{1,*}

¹Department of Physiology, Anatomy and Genetics, University of Oxford, South Parks Road, Oxford OX1 3QX, UK

²Nuffield Department of Clinical Neurosciences, Academic Unit of Neuropathology, University of Oxford, John Radcliffe Hospital, Oxford OX3 9DU, UK

³The Oxford Parkinson's Disease Centre, University of Oxford, Oxford OX1 3QX, UK

⁴Sir William Dunn School of Pathology, University of Oxford, South Parks Road, Oxford OX1 3RE, UK

*Correspondence: richard.wade-martins@dpag.ox.ac.uk (R.W.-M.), tara.caffrey@dpag.ox.ac.uk (T.M.C.)

<http://dx.doi.org/10.1016/j.stemcr.2017.06.005>

SUMMARY

The H1 haplotype of the microtubule-associated protein tau (*MAPT*) locus is genetically associated with neurodegenerative diseases, including Parkinson's disease (PD), and affects gene expression and splicing. However, the functional impact on neurons of such expression differences has yet to be fully elucidated. Here, we employ extended maturation phases during differentiation of induced pluripotent stem cells (iPSCs) into mature dopaminergic neuronal cultures to obtain cultures expressing all six adult tau protein isoforms. After 6 months of maturation, levels of exon 3+ and exon 10+ transcripts approach those of adult brain. Mature dopaminergic neuronal cultures display haplotype differences in expression, with H1 expressing 22% higher levels of *MAPT* transcripts than H2 and H2 expressing 2-fold greater exon 3+ transcripts than H1. Furthermore, knocking down adult tau protein variants alters axonal transport velocities in mature iPSC-derived dopaminergic neuronal cultures. This work links haplotype-specific *MAPT* expression with a biologically functional outcome relevant for PD.

INTRODUCTION

Chromosome 17q21 represents an interesting genomic locus featuring an ~1.3–1.6 Mb region of linkage disequilibrium (LD) encompassing the microtubule-associated protein tau (*MAPT*) gene, including genetic variants associated with several neurodegenerative disorders. The LD surrounding *MAPT* is due to a 900 kb chromosomal inversion proposed to originate from non-allelic homologous recombination between long coding repeats flanking the region (Cruts et al., 2005), giving rise to two correspondingly large haplotype families called H1 and H2. The *MAPT* gene is of central importance to a number of neurodegenerative diseases. Strong association of *MAPT* H1 haplotype variants has been shown with progressive supranuclear palsy (PSP) (Hoglinger et al., 2011), corticobasal degeneration (CBD) (Kouri et al., 2015), and Parkinson's disease (PD) (Nalls et al., 2014).

The *MAPT* gene is characterized by diversity at the transcript and protein level. The gene expresses six transcripts through the alternative splicing of exons 2, 3, and 10 resulting in six major tau protein isoforms in the adult CNS (Andreadis et al., 1992; Goedert et al., 1989). Splicing of exons 2 and 3 yields proteins with 0, 1, or 2 N-terminal inserts (0N, 1N, and 2N tau). Exclusion or inclusion of exon 10 alters the number of microtubule binding repeats to give three or four microtubule binding repeats (3R or 4R tau). Expression of tau protein isoforms shows brain region specificity (Caffrey et al., 2006; Majounie et al., 2013; Trabzuni et al., 2012) and is regulated during development,

with roles in establishing and maintaining neuronal morphology. Importantly, tau proteins have been shown to aggregate in those brain regions that degenerate in a number of diseases, collectively referred to as tauopathies. Tauopathies show differing aggregation compositions of tau protein, with principally 4R tau aggregating in PSP, CBD, and frontotemporal dementia with Parkinsonism associated with chromosome 17 (FTDP-17) (Arai et al., 2001; Buee Scherrer et al., 1996); 3R tau proteins aggregating in Pick's disease (Delacourte et al., 1996); and both 3R and 4R tau aggregating in Alzheimer's disease (Sergeant et al., 1997; Williams, 2006). Despite having a strong genetic association with *MAPT*, PD does not typically give rise to tau tangle pathologies.

While *MAPT* coding and splice site mutations have been shown to be sufficient to cause FTDP-17, the *MAPT* haplotype variants do not encode protein changes that could underlie the genetic association. We and others have previously studied haplotype effects on gene expression at the *MAPT* locus (Caffrey et al., 2006, 2008; Kwok et al., 2004; Majounie et al., 2013; Trabzuni et al., 2012). Our studies have shown that the H2 haplotype expresses twice as much exon 2+3+ *MAPT* transcript as H1 (Caffrey et al., 2008), a finding that has been replicated in a large post-mortem brain series (Trabzuni et al., 2012). In addition, we showed that the *MAPT* H1 haplotype expresses 40% more exon 10+(4R) *MAPT* transcript than H2 (Caffrey et al., 2006), and this difference in exon 10+ transcript expression was greater in the globus pallidus than in the frontal cortex, demonstrating a mechanistic link between



the regulation of *MAPT* gene expression by disease-associated polymorphisms and the regional vulnerability exhibited in PSP, a 4R-tauopathy. A previous report has found an increase in the ratio of 4R:3R *MAPT* transcripts in PD brains (Tobin et al., 2008), potentially suggesting a shared mechanism of disease.

Induced pluripotent stem cell (iPSC)-derived neuronal cultures provide a powerful and tractable human neuronal model generated directly from individuals with disease, or harboring specific genetic variants. A major advantage of iPSC-derived neuronal cultures is the use in experimental studies of a key cell type of interest, enabling experimental analysis in living human neurons in a manner not attainable using postmortem tissues (Fernandes et al., 2016; Hartfield et al., 2014). Here, we differentiated dopaminergic neuronal cultures from iPSC lines heterozygous for the *MAPT* H1/H2 haplotypes to assess the effect of *MAPT* haplotype on gene expression and the role of tau protein isoforms in dopamine neurons preferentially vulnerable to degeneration in PD. iPSC-derived dopaminergic neuronal cultures express all six adult tau isoforms, approaching adult levels of expression of exon 3+ and exon 10+ transcripts after 6 months of maturation. This model was shown to be suitable to study both common genetic variations, displaying significant haplotype-specific differences in *MAPT* expression and splicing, as well as being able to characterize the effects of a rare genetic polymorphism on splicing. Finally, we perturbed the expression of both total and 4R tau in iPSC-derived dopamine neurons to demonstrate that tau isoforms regulate axonal transport velocity, linking genetic variation, gene expression, and splicing with neuronal function.

RESULTS

Establishment of Human Dopaminergic Neuronal Cultures that Express Adult Tau Isoforms

To study the relationship between genetic variation at the *MAPT* locus and PD we used human iPSCs to generate dopamine neurons from individuals carrying specific genotypes of interest. As any effect of underlying genetic polymorphic variation on gene expression and splicing is independent of disease status, we chose to use control individuals of known genotype for this study. In addition, by using individuals heterozygous for *MAPT* H1/H2, we are able to assay expression from both haplotypes in one culture controlling for confounding factors such as different genetic backgrounds, culture conditions, or environmental factors. Fifty-eight healthy controls from the Oxford Parkinson's Disease Center Discovery Cohort were screened to identify individuals heterozygous for the *MAPT* H1 and H2 alleles. Of the 58 individuals genotyped, 38%

were the desired H1/H2 genotype, 53% were H1/H1, and 9% were H2/H2. Fibroblasts from H1/H2 individuals were reprogrammed to generate iPSC clones, some of which have been described previously (Dafinca et al., 2016; Hartfield et al., 2014; Sandor et al., 2017) (see also Table S1). Characterization of the new iPSC clones is presented in Figures S1 and S2. In total, eight iPSC clones made from three H1/H2 individuals were selected for use in this study (Figure 1A, see also Table S1).

Differentiation of iPSCs toward a midbrain fate generated dopaminergic neuronal cultures expressing neuron-specific beta-III tubulin (β 3-tub) and the dopaminergic neuronal marker tyrosine hydroxylase (TH), identified by western blot (Figure 1B) and immunocytochemistry (Figures 1C and 1D). Approximately 65% of cells were β 3-tub positive, with up to 60% of those co-expressing TH (Figure 1C).

Expression of the *MAPT* gene is both spatially and developmentally regulated, and it is primarily expressed in neurons. Adult human brain shows expression of six principal isoforms generated through the splicing of exons 2, 3, and 10 (Andreadis et al., 1992; Goedert et al., 1989), while the human fetus expresses only the shortest isoform, lacking exons 2, 3, and 10. To characterize the maturity of our dopaminergic neuronal cultures with respect to *MAPT* expression, we examined the expression of these isoforms over a 24-week (to 188 days *in vitro* [DIV188]) time course of maturation of iPSC-derived differentiation cultures using real-time qPCR. During this period the relative expression of total *MAPT* transcripts peaked at DIV48 (4 weeks after re-plating) (Figure 2A, see also Figure S3B). By maturation to DIV188, cultures exhibited a 15-fold increase in the expression of adult isoforms containing exon 3 (Figure 2B) and a 7-fold increase in the expression of adult isoforms containing exon 10 (Figure 2C), both clear evidence of neuronal maturation. Cultures maintained in culture to DIV188 reached an inclusion level of exon 3 (encoding 2N tau protein isoforms) similar to levels in postmortem human midbrain (iPSC-derived cultures, 5.6%, Figure 2B; midbrain, 6.8%, Figure 2D). At the same time point, the inclusion of exon 10 (corresponding to the 4R tau protein isoforms) had risen toward the level of inclusion measured in postmortem human midbrain (iPSC-derived cultures, 18.2%, Figure 2C; compared with midbrain at 35.2%, Figure 2D).

Dopaminergic neuronal cultures of all eight iPSC lines were matured for 6 months (DIV190) to give mature inclusion of adult-specific exons in *MAPT* transcripts. Western blot analysis of 6-month cultures revealed that the inclusion of exons 3 and 10 at the transcript level led to the presence of all six isoforms of tau protein, detected by either a pan-tau antibody or antibodies probing for 4R and 2N tau isoforms (Figure 3). Tau protein was not detected by the

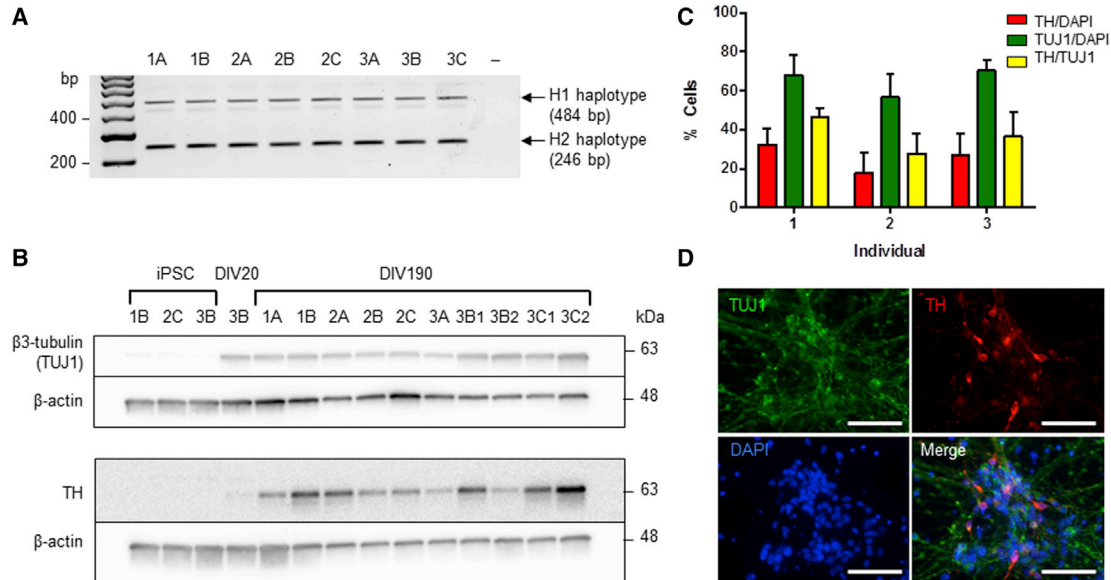


Figure 1. Differentiation of Induced Pluripotent Stem Cells with *MAPT* H1/H2 Genotype into Dopaminergic Neuronal Cultures

(A) Genotyping PCR distinguishes the 238 bp indel in *MAPT* intron 9, showing the presence of both the H1 and H2 alleles in all eight iPSC clones. Clones are identified by the number of the individual (1–3) then by the clone generated from reprogramming of the fibroblasts of that individual (A–C).

(B) Western blots showing iPSC differentiation into dopamine neuronal cultures. Neuronal marker β3-tubulin (TUJ1) (expressed by DIV20) and tyrosine hydroxylase (TH) are shown at DIV190. Samples from two differentiations are identified by a “1” or “2” suffix.

(C) Efficiency of dopaminergic differentiation was quantified from at least two clones per individual. Individuals differentiated with similar efficiencies into neurons determined by TUJ1/DAPI. The proportion of neurons that were dopaminergic was determined by TH/TUJ1. Mean ± SEM of $n = 2$ or 3 clones per individual; 4 images per clone.

(D) Immunofluorescent co-labelling of differentiated neuronal cultures from clone 3B fixed at DIV27 (1 week after re-plating) demonstrates expression of dopaminergic neuronal protein TH together with β3-tubulin. Scale bars, 50 μm. See also Figures S1 and S2.

antibody Tau-1 in iPSCs before commencing differentiation (Figure 3, lanes 2–4). After running this blot, one particular batch of iPSC line 1A (lane 6) was discovered to have a duplication in chromosome 1q and was removed from further analysis. Overall, these data show that, by 6 months, iPSC-derived dopaminergic neuronal cultures show significant adult-like maturity, recapitulating expression patterns seen in adult midbrain, and represent a promising model for the study of *MAPT* biology.

Haplotype-Specific Expression of *MAPT* in Human Dopaminergic Neuronal Cultures

We used our model to investigate the haplotype-specific expression of *MAPT* in dopamine neurons, the neuronal type that is preferentially vulnerable in PD. Samples from the same 6-month neuronal cultures of the eight heterozygous H1/H2 iPSC lines shown above were analyzed by real-time qPCR. The levels of total *MAPT* transcripts showed no significant difference between individuals (Figure 4A). Transcripts containing exon 3 also showed no significant difference between individuals, with the average inclusion of exon 3 for all eight lines being 9.1% (Figure 4B). How-

ever, individual 3 showed a significantly higher inclusion of exon 10 in *MAPT* transcripts (22%) compared with individuals 1 (16%) and 2 (15%) ($p = 0.0005$) (Figure 4B).

The high levels of mature *MAPT* exons 3 and 10 inclusion allow the development of allele-specific expression assays to distinguish the relative abundance of H1 and H2 transcripts using a SNP. We developed a set of TaqMan-based real-time qPCR allele-specific expression assays using SNPs in exon 1 (rs17650901) and exon 9 (rs17652121) of *MAPT* to distinguish between transcripts deriving from H1 and H2 alleles (Figure 4, see also Figures S3C–S3F). The output of these assays is the ratio of H1:H2 transcripts for a given PCR amplicon, in which a ratio greater than 1 represents more expression from the H1 allele than from the H2 allele, and a ratio less than 1 represents more expression from the H2 allele than from the H1 allele.

The expression of all *MAPT* transcripts combined, measured by amplifying transcripts between constitutive exons 0 and 1, was 23% greater from H1 than from H2 in DIV190 dopaminergic neuronal cultures (Figure 4C) ($p < 0.0001$), with significantly greater H1 expression also seen at DIV124 (11%; $p = 0.0132$) and DIV188 (31%; $p < 0.0001$)

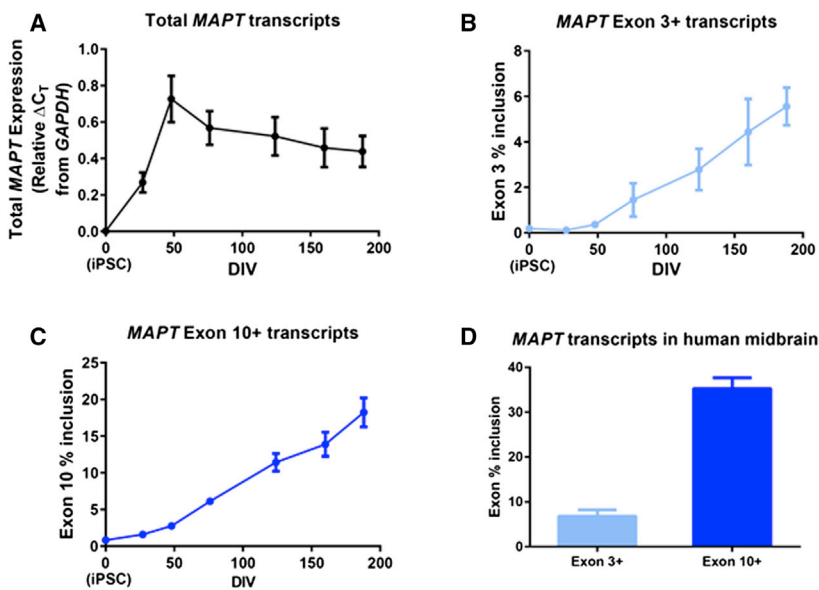


Figure 2. MAPT Adult Isoforms Increase in Expression over a 6-Month Differentiation

(A–C) Real-time qPCR analysis demonstrated changes in *MAPT* expression over 24 weeks of maturation to DIV188. Each graph shows mean \pm SEM, $n = 7$ clones (all clones except 1A). At DIV188, peak mean inclusion for the alternatively spliced exons 3 and 10 was 5.6% (B) and 18.2% (C), respectively. For each graph (A–C), linear regression performed using all data points from DIV48 to DIV188 with an F test confirming that each slope is significantly different from zero: (A) $y = -0.01303 \times x + 0.7279$, $F = 4.615$, $p = 0.0391$; (B) $y = 0.2553 \times x - 0.7078$, $F = 23.32$, $p < 0.0001$; (C) $y = 0.7416 \times x - 0.05151$, $F = 96.28$, $p < 0.0001$.

(D) Exon inclusion from TaqMan-based real-time qPCR expression assays performed on human midbrain cDNA. Mean \pm SEM, $n = 5$ individuals; exon 3+ mean = 6.79 ± 1.43 ; exon 10+ mean = 35.22 ± 2.43 . See also Figure S3.

in the time course sample set (Figure S4). In the same assay, total *MAPT* expression in postmortem human midbrain did not differ significantly from an allelic ratio of 1 (Figure 4C).

The average H1:H2 allelic ratio of *MAPT* transcripts containing exon 3 was 0.56 across all iPSC-derived dopaminergic culture sample sets, closely matching that of 0.51 in the midbrain sample set (Figure 4D, see also Figure S4B). This demonstrates that the H2 allele expresses approximately twice as many *MAPT* transcripts containing exon 3 as the H1 allele. These exon 3 expression data from dopaminergic neuronal cultures and midbrain agree with those of postmortem brain tissue and other neuronal models studied previously (Caffrey et al., 2008; Trabzuni et al., 2012).

Finally, the allelic ratios of *MAPT* transcripts containing exon 10 were not different from 1 for DIV190 dopaminergic neuronal cultures from individuals 1 and 2 (Figure 4E). However, cultures from individual 3 showed a marked shift to a ratio of 0.51 (Figure 4E, see also Figures S4C and S4D), which we investigated further below. Consistent with previous observations in postmortem brain tissue and other neuronal models (Caffrey et al., 2006), but differing from our iPSC-derived dopaminergic neuronal cultures, postmortem human midbrain exhibited an H1:H2 ratio for exon 10+ transcripts of 1.2 (Figure 4E).

In summary, our iPSC-derived dopaminergic neuronal culture model recapitulates the allele-specific expression differences previously seen in human brain for exon 3, exhibiting a 2-fold increase from H2. Although we observed an increased total *MAPT* expression associated with the H1 *MAPT* haplotype as reported previously (Allen et al., 2014; Kwok et al., 2004), we did not observe changes in

exon 10+ expression associated with *MAPT* haplotype. Interestingly, our iPSC-derived neuronal cultures permitted the observation of a further expression phenotype in the iPSC lines from individual 3.

Identification of a Genetic Variant that Alters the Inclusion of MAPT Exon 10

We noted that the *MAPT* exon 10 expression in dopaminergic neuronal cultures from the three iPSC clones from individual 3 was significantly different to neurons studied from five lines generated from individuals 1 and 2. Dopaminergic neuronal cultures generated from individual 3 showed an overall 40% increase in inclusion of exon 10 (Figure 4B) and a 2-fold increase in expression of exon 10+ transcripts, specifically from the H2 allele (Figure 4E). To investigate these expression phenotypes further, *MAPT* exons 9 and 10 and their flanking regions were sequenced. Individuals 1 and 2 showed the expected wild-type (WT) sequence; however, an indel was detected in individual 3 that resulted in a divergent sequence 102 bp downstream of exon 10 (Figure 5A). Primers placed in or adjacent to the haplotype-tagging 238 bp indel in intron 9 were used to specify the allele to be amplified by PCR and each chromosomal locus was subcloned and sequenced. A deletion of three nucleotides was identified in intron 10 (c.1919+102_1919+104delCTT, hereafter Δ CTT) only in the H2 allele of individual 3 and not on either allele of in individuals 1 and 2 (Figure 5B). This Δ CTT variant does not exist on public databases of genetic variation (www.ncbi.nlm.nih.gov/variation/view/), (www.ncbi.nlm.nih.gov/SNP/[Sherry et al., 2001]). As the deletion was present on the allele that showed increased exon

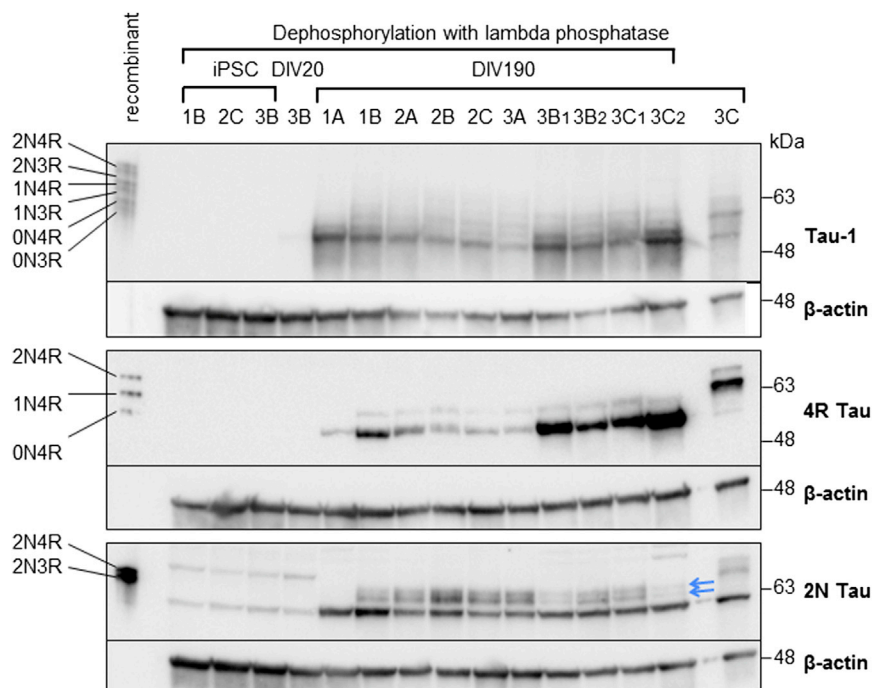


Figure 3. All Major Tau Protein Isoforms Are Expressed in iPSC-Derived Dopaminergic Neuronal Cultures Differentiated for 6 Months

Western blots showing the presence of all six major isoforms of mature tau protein in dopaminergic neuronal cultures at DIV190, as detected by antibodies against total tau (Tau-1) or specific isoforms (4R Tau, 2N Tau). All samples dephosphorylated, except the right lane as an untreated control. 2N Tau blot: central bands indicated by blue arrows represent the two 2N Tau isoforms. Additional bands are considered non-specific as they appear in the iPSC lysate in which no tau is detectable.

10 inclusion, this strongly suggests that the Δ CTT variant causes increased inclusion of exon 10 in agreement with the altered H1:H2 exon 10 inclusion ratio.

To examine possible functional mechanisms for the increased inclusion of exon 10 in transcripts that include the Δ CTT variant, an *in silico* search of splice factor binding sites was performed on the intronic sequence with or without the Δ CTT variant using *SpliceAid 2* (Figure 5, see also Figure S5) (Piva et al., 2012). Searching for all available splicing factors, two binding sites were predicted to be lost by the Δ CTT variant: RBM4, which is predicted to enhance inclusion of exon 10 (Kar et al., 2006), and PTBP1 (PTB/hnRNP I), which is predicted to promote exclusion of exon 10 (Wang et al., 2004). In the presence of the Δ CTT variant, the predicted binding site for RBM4 would be reduced from 9 to 6 bp, and that of PTBP1 from 6 to only 3 bp. Real-time qPCR for *RBM4* and *PTBP1* confirmed the expression of both of these splicing factors in cultures of clones from each of the three individuals across the period of the time course (Figures S5C and S5D). Furthermore, the expression of *RBM4* and *PTBP1* appears to be correlated in these samples (Figure S5E). From DIV48, the expression levels of both genes appears to be relatively stable, rather than matching the observed increase in inclusion of exon 10 over time. Importantly, although there was a clear difference in *MAPT* exon 10 inclusion between individual 3 and individuals 1 and 2 (Figure S5F), there was no difference in the expression of *RBM4* and *PTBP1* in the clone from individual 3 when compared with clones from individuals 1

and 2, showing that there is no intrinsic difference in the expression of these splicing factors that could otherwise explain the phenotype of individual 3.

We performed RNA-electrophoretic mobility shift assays to study the impact of the Δ CTT sequence on RNA-protein complex formation between biotinylated RNA probes containing the exon 10 WT or Δ CTT sequence and SK-N-F1 nuclear protein extract (Figure 5C). Four RNA-protein complexes (I–IV) were formed using the WT RNA probe (Figure 5C, lane 2), while only three (II–IV) were visible when the CTT sequence was deleted (Figure 5C, lane 8), indicating that the CTT deletion reduced the number of species of protein complexes interacting with the RNA. The band shift intensities of the WT sequence and nuclear extract were much stronger than those observed for the Δ CTT sequence (Figure 5C, lanes 2 and 8), suggesting that the CTT sequence forms part of an important RNA motif for protein binding. We further assessed the binding strengths of the WT and Δ CTT sequences by competition experiments in which unlabeled RNA oligonucleotides competed with the probes for complex formation (Figure 5C, lanes 3–6, 9–12). The Δ CTT competitor showed a reduced competition strength compared with the WT competitor when assayed with the WT probe for complex formation (Figure 5C, lanes 3–6), whereas the two competitor oligonucleotide sequences exhibited comparable competition strength with the Δ CTT probe (Figure 5C, lanes 9–12).

We probed for interaction of PTBP1 and RBM4 after pull-down of nuclear proteins with the WT or Δ CTT probes

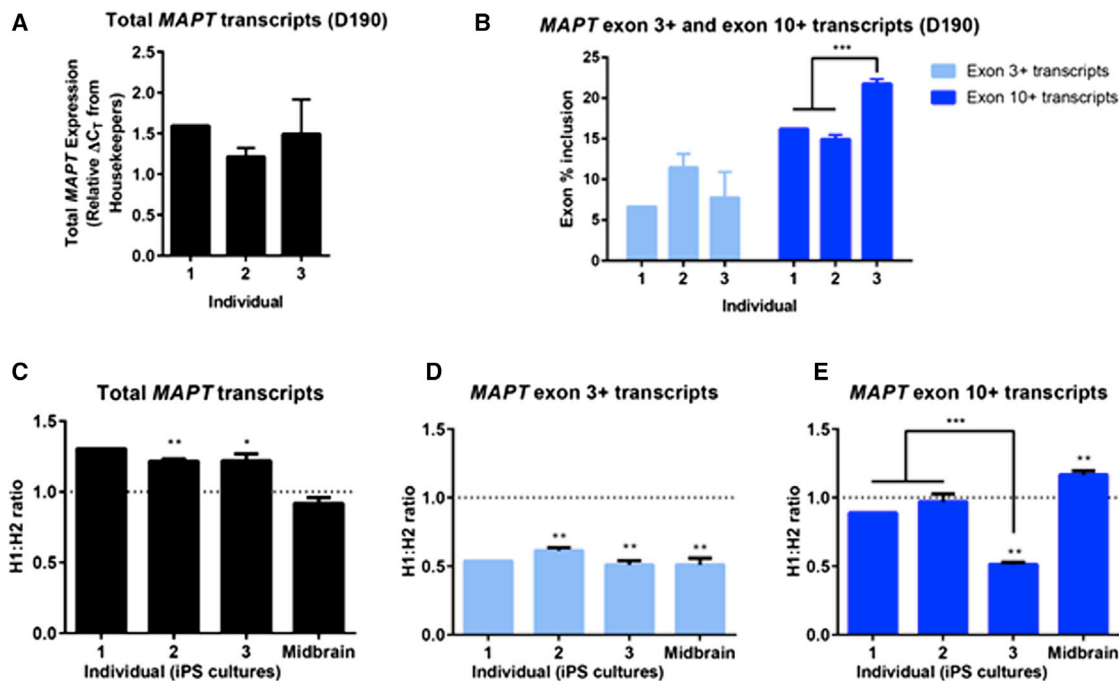


Figure 4. Dopaminergic Neuronal Cultures Exhibit Significant Differences in Isoform Expression from H1 and H2 Alleles at 6 Months

TaqMan-based real-time qPCR expression assays on samples at DIV190. Mean \pm SEM; individual 1, n = 1 clone; individuals 2 and 3, n = 3 clones; ≥ 3 cDNA samples per clone.

(A) Total *MAPT* expression reported as relative ΔC_T of geometric mean of three housekeeper genes (*GAPDH*, *HPRT1*, and *ACTB*). n.s., not significant, one-way ANOVA.

(B) Percent inclusion of alternatively spliced exons 3 (light blue) and 10 (dark blue) at DIV190. The three individuals show similar inclusion of exon 3, whereas individual 3 shows a significantly greater inclusion of exon 10. Significant difference between groups in an unpaired t test: ***p = 0.0005.

(C–E) Allele-specific expression assays distinguishing transcripts of H1 and H2 allelic origin, presented as H1:H2 ratio, i.e., values >1 show higher H1 expression. Data from analysis of human midbrain (C) n = 9; (D) n = 5; and (E) n = 9. (C) Individuals 2 and 3 show significantly greater expression of total *MAPT* transcripts from the H1 chromosome (individual 2, **p = 0.0059; individual 3, *p = 0.0471; midbrain, n.s.). (D and E) The H1:H2 ratio is normalized to the H1:H2 ratio of total *MAPT* transcripts per sample. *Significant difference from mean of 1 in a one-sample t test. (D) There are 2-fold greater exon 3-containing transcripts coming from the H2 chromosome. Individual 2, **p = 0.0032; individual 3, **p = 0.0040; midbrain, **p = 0.0020. (E) Haplotype-specific expression of exon 10 varies between individuals and midbrain: Individual 2, n.s.; individual 3, ***p = 0.0008; midbrain, **p = 0.0005. Significant difference between groups in an unpaired t test: ***p = 0.0005. See also [Figures S3](#) and [S4](#).

([Figure 5D](#)). Firstly, this technique successfully shows an interaction of PTPB1 with both probes, whereas the signal for RBM4 rose barely above background despite robust presence in the starting lysate. Secondly, the PTPB1 interaction with the Δ CTT variant is greatly reduced compared with the WT sequence. The results indicate that a CTT deletion in this region could potentially reduce the binding of RNA binding proteins such as PTPB1, thereby altering the balance of exon 10 inclusion and exclusion in transcripts.

Tau Knockdown Alters Velocity of Axonal Transport in Human Dopaminergic Neuronal Cultures

The *MAPT* H1 allele is established to carry risk for PD, and we describe above an increased allelic expression of

total *MAPT* transcripts in dopaminergic neuronal cultures compared with the protective H2 allele ([Figure 4C](#)). Furthermore, our postmortem human midbrain samples confirmed increased expression of exon 10+ *MAPT* transcripts from the H1 allele ([Figure 4E](#)). We note that both of these scenarios would contribute to having more molecules of 4R tau protein present in cells carrying the H1 allele. We therefore developed a dual approach to investigate the functional effect of 4R tau expression in dopaminergic neuronal cultures. We hypothesized that a decrease in the level of total tau expression, or 4R tau expression, both of which mimic the protective H2 condition, may be beneficial to dopamine neurons. We designed short hairpin RNAs (shRNAs) to target either a constitutive

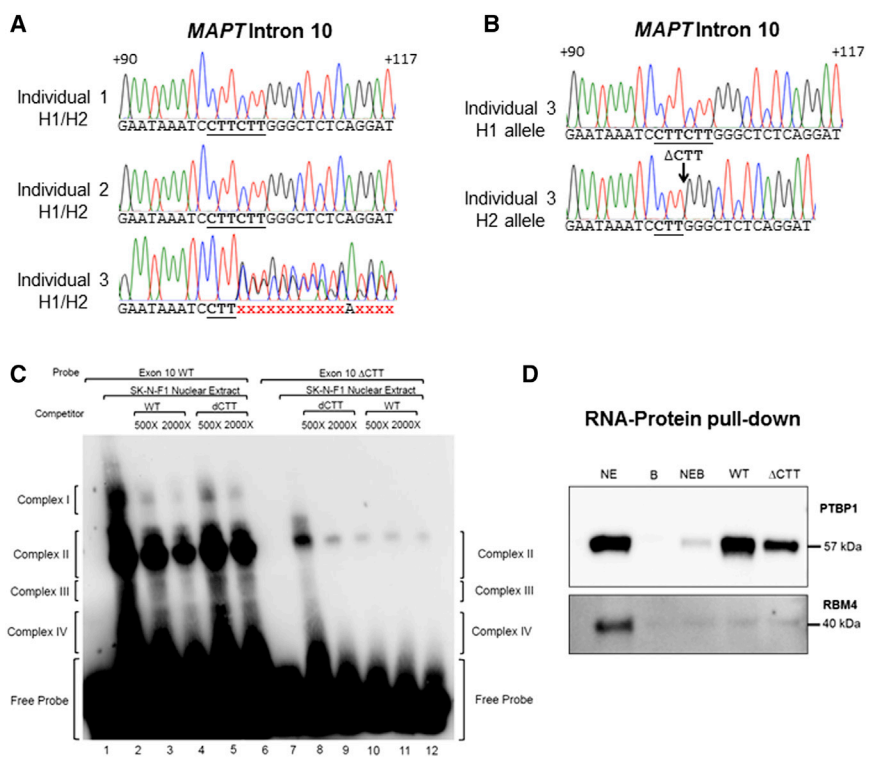


Figure 5. A Deletion in *MAPT* Intron 10 Decreases Binding of Factors that Regulate Exon 10 Splicing

(A) Sequencing chromatograms for *MAPT* intron 10 showing the expected sequence for genomic DNA (both H1 and H2 alleles together) for individuals 1 and 2. The red x's represent divergent chromatograms from two overlapping sequences caused by an indel on one allele for individual 3. (B) Sequencing chromatograms for *MAPT* intron 10 showing single allelic genomic DNA from individual 3. The H2 allele showed a Δ CTT variation. (C) Electrophoretic mobility shift assay using an RNA probe for an intron 10 wild-type (WT) sequence (lanes 1–6) and an RNA probe for an intron 10 Δ CTT variant sequence (lanes 7–12), with and without competitors. (D) Western blot of RNA-protein pull-down using the WT and Δ CTT RNA probes. Lanes indicate proteins obtained from nuclear extract only (NE), beads only (B), NE and B (NEB), WT RNA probe and the Δ CTT probe. Blots are shown for PTPB1 and RMB4. See also Figure S5.

exon of *MAPT* (i.e., all transcripts), or targeted specifically at *MAPT* transcripts including exon 10, or a scrambled shRNA not matching any known RefSeq transcript. These three shRNA sequences were incorporated into lentiviral plasmids. Following transduction at DIV20 shortly after re-plating, dopaminergic neuronal cultures were matured for either 4 weeks or 5 months. Tau protein was knocked down by 65% at 4 weeks (Figure 6A), with knockdown persisting at 5 months post-transduction (Figure 6B), while maintaining expression of the blue fluorescent protein (EBFP2) reporter (Figure 6C). The shRNA targeting *MAPT* exon 10 efficiently knocked down 4R tau protein in 5-month cultures (Figure 6B). Cultures were incubated with MitoTracker Deep Red to enable visualization of mitochondria for live fluorescence imaging (Figure 6D). After using the EBFP2 reporter to identify transduced neurons, analysis of kymographs generated from time-lapse imaging enabled measurement of the velocity of mitochondria (Figure 6E).

When compared with the scrambled shRNA control, there was no significant difference in mitochondrial velocity when tau protein was reduced in young neurons (4 weeks post-transduction; Figure 6F, upper). However, in older neurons (5 months post-transduction) where the complement of tau proteins is more representative of expression in the adult human brain, knockdown by the 4R *MAPT* shRNA caused a significant increase in median mitochondrial velocity from 0.148 to 0.574 μ m/s (adjusted

$p = 0.0007$; Figure 6F, lower left). Furthermore, when the period during which a mitochondrion has paused is removed from the calculations for average velocity, both knockdown conditions (4R and total *MAPT*) produced a significant increase in median mitochondrial velocity compared with the scrambled shRNA control, from 0.272 μ m/s for scrambled to 0.793 and 0.519 μ m/s for 4R and total *MAPT* knockdown, respectively (4R *MAPT* adjusted $p = 0.0002$; total *MAPT* adjusted $p = 0.0191$; Figure 6F, lower right). As the level of total tau protein is similar between the two knockdown conditions, these data suggest that the disruption of the balance of 4R and 3R tau isoforms is what is giving rise to the most significant differences in mitochondrial velocity. This increase remains, and is reinforced, after removal of pause periods, suggesting that the alteration in velocity is not simply due to a reduction in the chance of a mitochondrion stalling/pausing, but to an intrinsic increase in the velocity of axonal transport.

Due to the requirement for high-density cultures to generate TH+ dopaminergic neurons, it was not possible to determine transport direction in our assay system as axons were not able to be assigned to specific cell bodies. Kinesin produces movement solely in the anterograde direction, whereas cytoplasmic dynein, while predominantly a retrograde motor, is capable of reversing and so functions bidirectionally (Dixit et al., 2008), so we therefore stratified the data by separating mitochondria that had >90% of their

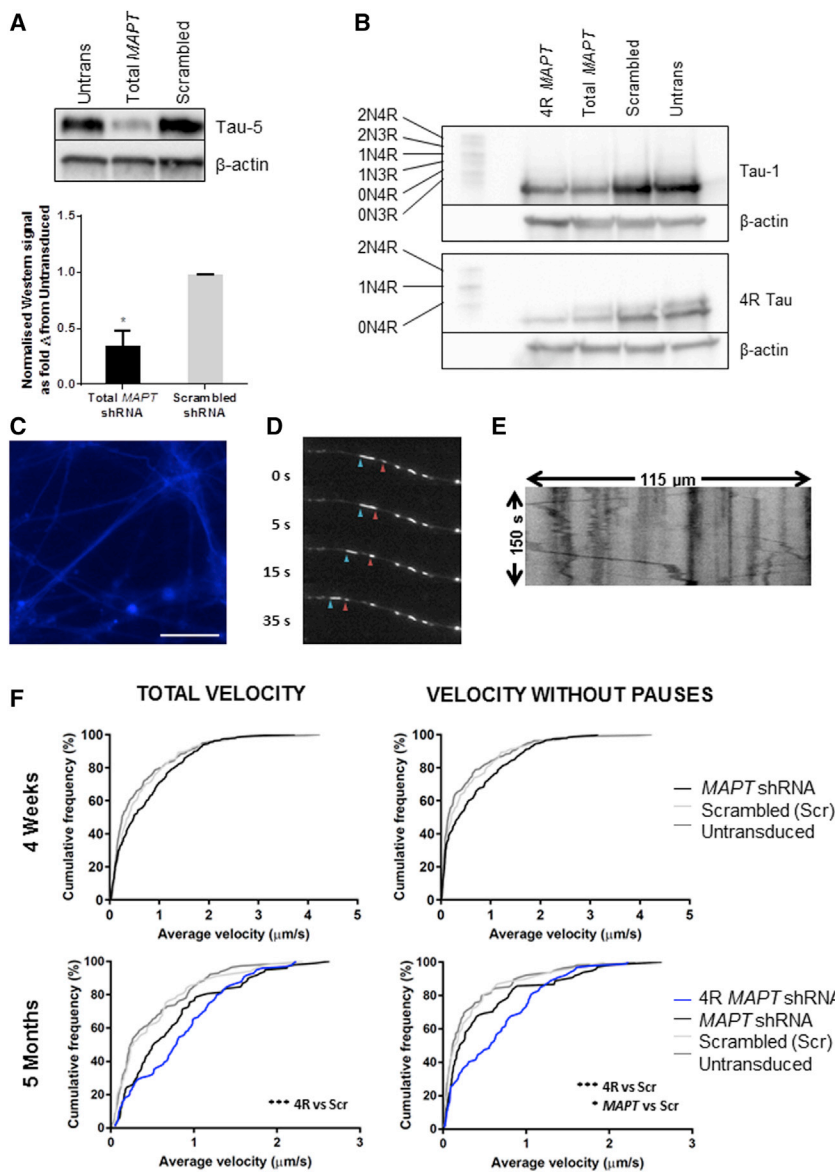


Figure 6. Knockdown of 4R Tau Increases Velocity of Mitochondrial Axonal Transport in iPSC-Derived Dopaminergic Neuronal Cultures Differentiated for 5 Months

(A) Western blots showing knockdown of tau protein in dopaminergic neuronal cultures 4 weeks post-transduction. * $p = 0.0457$.

(B) Western blots after protein dephosphorylation show knockdown of tau protein and 4R tau isoforms persisting in 5-month dopaminergic neuronal cultures with β -actin loading control.

(C) Fluorescence microscopy image of EBFP2 expression during axonal transport live imaging at 5 months. Scale bar, 25 μ m.

(D) Selected time-lapse fluorescence microscopy images of axonal mitochondria in dopaminergic neuronal cultures stained with MitoTracker Deep Red. Arrowheads show motile mitochondria.

(E) Kymograph time-space plot of a trace along the linear path of an axon, from which mitochondrial motility parameters can be determined.

(F) Cumulative frequency graphs of average mitochondrial velocity in dopaminergic neuronal cultures at (top) 4 weeks post-transduction and (bottom) 5 months post-transduction. (Left) Average total velocity of each measured motile mitochondrion; (right) average velocity of each measured motile mitochondrion after removal of time when paused. All four graphs were statistically significant in Kruskal-Wallis nonparametric tests: upper left, $p = 0.0033$; upper right, $p = 0.0200$; lower left, $p < 0.0001$; lower right, $p < 0.0001$. *Significance in the follow-up Dunn's multiple comparisons test (nonparametric) compared with scrambled shRNA control: * $p < 0.05$; *** $p < 0.001$. See also Figure S6.

movement in a single direction (unidirectional) from those that were bidirectional. In young neurons, no significant difference was observed between knockdown and scrambled conditions. In older neurons, knockdown of 4R tau resulted in a significant increase in velocity for mitochondria moving in one direction only, with or without inclusion of paused periods (Figure S6E: $p = 0.0048$; Figure S6F, $p = 0.0033$), but showed no difference in velocity of bidirectional mitochondria (Figures S6G and S6H), showing that the overall effect seen by 4R tau knockdown was carried by unidirectional mitochondria. In contrast, knockdown of total tau resulted in increased velocity of both unidirectional and bidirectional mitochondria, but only when pause periods were removed (Figure S6F, $p = 0.0078$; Fig-

ure S6H $p = 0.0327$). These data suggest tau regulates kinesin anterograde transport to a greater extent than dynein anterograde transport.

DISCUSSION

In this work, we have established an iPSC-derived dopaminergic neuronal cell culture model suitable for the study of the expression and function of MAPT in those neurons preferentially vulnerable to neurodegeneration in PD. We have shown that iPSC-derived dopaminergic neuronal cultures expressing a high level of the neuronal markers β 3-tub and TH show increasing expression of adult tau



isoforms throughout the maturation phase. Notably, levels of expression of exon 3+ and exon 10+ transcripts approach adult levels after 6 months of neuronal maturation, with strong expression of 2N and 4R tau protein isoforms evident. This highly physiological *MAPT* expression profile makes iPSC-derived dopaminergic neurons a highly suitable system to study the genetic regulation of tau expression in a tractable human dopamine neuronal culture model.

An important aspect of tau biology is the effect of *MAPT* genetic variation on the expression of tau isoforms. Discovery of exon 10 splice site mutations in pedigrees with FTDP-17 demonstrated for the first time that *MAPT* non-coding genetic variation changed the balanced expression of the 3R and 4R tau protein, and that the imbalanced expression was sufficient to cause disease (Hutton et al., 1998; Spillantini et al., 1998). Studies by our group (Caffrey et al., 2006, 2008) and others (Majounie et al., 2013; Trabzuni et al., 2012) have demonstrated that common *MAPT* genetic variation associated with disease alters the expression of tau transcripts and that this effect varies between brain regions. Combining these attributes of tau biology requires tau to be studied in a tractable model expressing the adult tau isoforms, such as iPSC-derived dopaminergic neuronal cultures.

Within the field of stem cell models of neurodegeneration, the age and maturity of iPSC-derived neuronal cultures is central to developing better models to study disease. *MAPT* isoform expression is developmentally regulated and therefore gives an excellent genetic marker of neuronal maturity. iPSC-derived dopaminergic neuronal cultures differentiated and matured using the protocol that we use here (Kriks et al., 2011) show increasingly more adult tau isoform expression over a maturation period of 6 months, with full-length 2N4R tau protein being detected at DIV190. Other studies of dopaminergic cultures detected mostly fetal tau present after 20 days in maturation medium (Ehrlich et al., 2015), which is in line with our findings. Similar expression patterns are noted in iPSC-derived cortical neuronal cultures. A detailed examination of tau proteins by mass spectrometry provided confirmation of the predominance of 0N3R tau peptides and the lack of peptides corresponding to exons 2 and 3 in 5-week iPSC-derived cortical neurons (Silva et al., 2016). Wray and colleagues (Sposito et al., 2015) noted that their iPSC-derived cortical cultures go through the developmental switch from fetal to adult tau after 365 days. Alteration of the developmental switch to adult tau isoforms occurs in cultures with tau mutations in which increased expression of 4R tau is observed at earlier time points than control (Ehrlich et al., 2015; Iovino et al., 2015; Silva et al., 2016; Sposito et al., 2015). Despite differences in cortical and dopaminergic differentiation protocols, it is clear that the

expression of the adult isoforms of tau requires extended periods of maturation. This is perhaps unsurprising considering the natural developmental switch of expression from fetal tau to adult tau over time in the human brain. As the tau isoform balance has proven key to the pathogenicity of splice site mutations in FTDP-17, and is a characteristic of the genetic association, the expression of the adult isoforms in neuronal cell culture models is vitally important for future tau biology work.

Our differentiated neuronal cultures allow us to investigate the effect of common genetic variation on *MAPT* expression. The allele-specific expression assays we developed detect differences in expression from the H1 and H2 haplotypes within heterozygous lines. We demonstrate that the dopaminergic neuronal cultures express 22% greater tau transcripts from the H1 chromosome than H2. This allelic difference in total tau expression has not been demonstrated in studies of postmortem tissue (Caffrey et al., 2006; Trabzuni et al., 2012), although other groups have reported it using genetic reporter constructs (Kwok et al., 2004). Whether this difference would change with even longer maturation phases is as yet unclear; however, we observe an increasing H1:H2 total tau over our time course. Interestingly, Hayesmoore et al. (2009) noted a negative correlation between H1:H2 total transcript ratio and age, indicating that age-related changes in haplotype expression are relevant in the human brain. When we examine the alternatively spliced *MAPT* transcripts at 6 months maturation, neurons possess a mature expression profile, recapitulating the 2-fold greater exon 3 containing transcripts from the H2 chromosome correctly mirroring expression in midbrain and other postmortem tissue regions (Caffrey et al., 2008; Trabzuni et al., 2012).

Our iPSC-derived dopamine neuronal cultures express exon 10 from the H1 and H2 chromosomes at equal ratio which differs from the ratio observed here in the midbrain tissue, as well as in previous publications of postmortem brain tissue (Caffrey et al., 2006; Majounie et al., 2013). It is possible this discrepancy arises due to the maturity or age of the culture as we document an increase in the expression of tau isoforms over extended maturation phases, although inclusion does not reach the 35% level seen in the midbrain samples. While the exon 10-containing transcripts maintain a similar H1:H2 transcript ratio throughout, it is possible that the ratios could change as exon 10 inclusion approaches the level of the adult midbrain. Alternatively, while this iPSC-derived model of dopaminergic neurons cultures provides a system in which to assay the function of the adult tau isoforms, it is possible that the culture system here may not support all the factors to recapitulate exon 10 inclusion as seen in the brain, which in turn would explain why the adult levels of exon 10 expression have not been achieved.



In our study we identified a rare non-coding variant within the *MAPT* locus. The previously undescribed Δ CTT variant occurring within intron 10 was found to alter the inclusion of exon 10 in transcripts and to change the balance of 4R tau protein isoforms. We observed a greater number of protein complexes bound the WT sequence than the Δ CTT variant, which agrees with in silico analysis predictions of the loss of two binding sites for RBM4 and PTBP1. We suggest that a partial loss of binding of RBM4 and a near abrogation of binding of PTBP1 would increase the likelihood of inclusion of exon 10 in transcripts originating from the Δ CTT H2 allele; alternatively, the loss of binding of both factors could alter the balance of remaining factors to promote exon 10 inclusion. The ability to assay the effect of genetic variation at the expression level is the first step in studying a range of tauopathies, from diseases caused by specific tau mutations such as those found in FTDP-17, to diseases with strong genetic associations with *MAPT* as in PD, PSP, and CBD.

It is clear from work on FTDP-17 splice site mutations (Hutton et al., 1998; Spillantini et al., 1998), as well as investigations into haplotype-specific expression of tau isoforms (Caffrey et al., 2006, 2008; Trabzuni et al., 2012), that the balance of tau isoform expression plays a major role in disease; however, the functional impact of subtle changes in expression brought about by common variants has yet to be fully investigated. The importance of the expression of alternative tau isoforms in the study of axonal transport was previously suggested by a study investigating the regulation of dynein and kinesin motor proteins. The longest tau isoform (2N4R) was shown to be a less potent inhibitor of both kinesin and dynein than the shortest tau isoform (0N3R) (Dixit et al., 2008). The high levels of adult tau isoform expression in our differentiated neuronal cultures allows us to investigate the effect of tau isoform expression on neuronal function. We have shown that depletion of 4R tau isoforms leads to increased axonal transport velocity in 5-month-old dopaminergic neuronal cultures. As this effect is strengthened after removal of pause periods it is likely that the alteration in velocity is not simply due to a reduction in the chance of a mitochondrion stalling/pausing, but to an intrinsic increase in the velocity of axonal transport. In addition, the effect of knockdown was greatest in mitochondria with unidirectional movement, which may support the data that indicate that tau affects kinesin anterograde movement greater than dynein (Dixit et al., 2008). We propose that the H2 haplotype, which expresses reduced 4R tau compared with the H1 haplotype, may exert a protective effect as it allows for more fluid mitochondrial movement along axons with high energy requirements, such as the dopaminergic neurons that degenerate in PD.

Advances in iPSC-derived neuronal models have opened up a new frontier for the study of human neurons as highly relevant genetic models, capturing the variants present in the donor. iPSC-derived dopaminergic neuronal cultures are known to be of high neurophysiological relevance (Hartfield et al., 2014) and reveal cellular phenotypes when comparing patients and controls (Fernandes et al., 2016) suitable for target and drug discovery. Here, we have been able to exploit iPSC-derived neurons to model the genetic basis of susceptibility to common disease by specifically choosing certain genotypes to functionally determine the effect of genetic variants on cell biology in the specific cell type of interest. Together, these attributes of iPSC-derived neuronal models demonstrate the great potential of studying neurons in a dish for future investigation into the genetic basis of neurodegenerative disorders.

EXPERIMENTAL PROCEDURES

iPSCs

All iPSC lines were derived from dermal fibroblasts from disease-free donors recruited through the Oxford Parkinson's Disease Center: participants were recruited to this study having given signed informed consent, which included derivation of hiPSC lines from skin biopsies (Ethics Committee: National Health Service, Health Research Authority, NRES Committee South Central, Berkshire, UK, who specifically approved this part of the study [REC 10/H0505/71]). All iPSC lines are detailed in [Supplemental Experimental Procedures](#), [Figures S1](#) and [S2](#); [Table S1](#).

Differentiation of iPSCs to Dopaminergic Neuronal Cultures

iPSCs were differentiated into dopaminergic neuronal cultures according to a modified protocol of Kriks et al. (2011) (see [Supplemental Experimental Procedures](#)). The medium was half changed every 2–3 days for the extended periods of maturation up to DIV190.

Allele-Specific Real-Time qPCR

Pairs of TaqMan probes were identified to distinguish the H1 and H2 alleles at *MAPT* SNP1 (rs17650901) and SNP9ii (rs17652121) (Myers et al. (2007)), and ordered as custom probe-only assays from Applied Biosystems. Validation of specificity was performed using H1/H1 or H2/H2 genomic DNA, followed by the generation of standard curves from 8:1 to 1:8 with *MAPT* H1 and H2 BAC constructs ([Figure S3](#)), which were adjusted through the origin.

Mitochondrial Axonal Transport Imaging

Cultures of iPSC-derived dopaminergic neuronal cultures were transduced with lentiviral particles encoding shRNAs on DIV20. Cultures were maintained until 4 weeks post re-plating or 5 months post re-plating before imaging. Cultures were incubated with MitoTracker Deep Red (Invitrogen) for 30 min then washed with Hank's



balanced salt solution with calcium and magnesium. Time-lapse imaging with Cy5 channel was performed using Volocity software to generate 150 images at 1-s intervals with 110-ms exposure (Vossel et al., 2015). Single EBFP2 images were taken on the DAPI channel to identify transduced neurons for each video.

Statistical Analysis

All statistical analysis and graphical representation was performed in Prism version 7 (GraphPad software). Specific tests are noted in each figure legend. For allele-specific expression studies, two-tailed one-sample *t* tests were used to determine whether the mean H1:H2 ratio was significantly different from 1. Unpaired two-tailed *t* tests were used to compare the expression levels of two groups. For axonal transport data, motile mitochondria from multiple imaging sessions were combined to produce a cumulative frequency (%) plot and analyzed by Kruskal-Wallis test with Dunn's multiple-testing correction. Knockdown conditions were compared with non-targeted shRNA conditions.

SUPPLEMENTAL INFORMATION

Supplemental Information includes Supplemental Experimental Procedures, six figures, and one table and can be found with this article online at <http://dx.doi.org/10.1016/j.stemcr.2017.06.005>.

AUTHOR CONTRIBUTIONS

J.E.B. designed and performed experiments, analysed data, and wrote the manuscript. M.C.L. and E.C. performed experiments. H.E.D.B. and F.Z. assisted in iPSC-derived differentiations and protocol development. L.P. provided post-mortem brain tissue. J.V. and S.A.C. generated and characterized the iPSCs. R.W.M. and T.M.C. funded the project, provided the concept, designed and interpreted experiments, and wrote the manuscript.

ACKNOWLEDGMENTS

The work was supported by the Monument Trust Discovery Award from Parkinson's UK. J.E.B. was supported by a Studentship from Parkinson's UK (H-1102). T.M.C. was supported by funds from IMI StemBANCC (no. 115439). We thank O. Cordero Llana for technical assistance. The research leading to these results has received support from the Innovative Medicines Initiative Joint Undertaking under grant agreement no. 115439, resources of which are composed of financial contributions from the European Union's Seventh Framework Program (FP7/2007–2013) and EFPIA companies. This publication reflects only the authors' views, and the IMI JU, EFPIA, and the European Commission are not liable for any use that may be made of the information contained therein. The Wellcome Trust (WTISSF121302) and The Oxford Martin School (LC0910-004) provide financial support to the James Martin Stem Cell Facility (to S.A.C.). We thank the High-Throughput Genomics Group at the Wellcome Trust Center for Human Genetics, Oxford (funded by Wellcome Trust grant reference 090532/Z/09/Z and MRC Hub grant G0900747 91070) for the generation of Illumina data. We acknowledge the Oxford Brain Bank, supported by the Medical Research Council (MRC), Brains for Dementia Research (BDR) (Alzheimer Society and Alzheimer

Research UK), Autistica UK, and the NIHR Oxford Biomedical Research Center.

Received: December 6, 2016

Revised: June 6, 2017

Accepted: June 6, 2017

Published: July 6, 2017

REFERENCES

- Allen, M., Kachadoorian, M., Quicksall, Z., Zou, F., Chai, H.S., Younkin, C., Crook, J.E., Pankratz, V.S., Carrasquillo, M.M., Krishnan, S., et al. (2014). Association of MAPT haplotypes with Alzheimer's disease risk and MAPT brain gene expression levels. *Alzheimers Res. Ther.* 6, 39.
- Andreadis, A., Brown, W.M., and Kosik, K.S. (1992). Structure and novel exons of the human tau gene. *Biochemistry* 31, 10626–10633.
- Arai, T., Ikeda, K., Akiyama, H., Shikamoto, Y., Tsuchiya, K., Yagishita, S., Beach, T., Rogers, J., Schwab, C., and McGeer, P.L. (2001). Distinct isoforms of tau aggregated in neurons and glial cells in brains of patients with Pick's disease, corticobasal degeneration and progressive supranuclear palsy. *Acta Neuropathol.* 101, 167–173.
- Buee Scherrer, V., Hof, P.R., Buee, L., Leveugle, B., Vermersch, P., Perl, D.P., Olanow, C.W., and Delacourte, A. (1996). Hyperphosphorylated tau proteins differentiate corticobasal degeneration and Pick's disease. *Acta Neuropathol.* 91, 351–359.
- Caffrey, T.M., Joachim, C., Paracchini, S., Esiri, M.M., and Wade-Martins, R. (2006). Haplotype-specific expression of exon 10 at the human MAPT locus. *Hum. Mol. Genet.* 15, 3529–3537.
- Caffrey, T.M., Joachim, C., and Wade-Martins, R. (2008). Haplotype-specific expression of the N-terminal exons 2 and 3 at the human MAPT locus. *Neurobiol. Aging* 29, 1923–1929.
- Cruts, M., Rademakers, R., Gijssels, I., van der Zee, J., Dermaut, B., de Pooter, T., de Rijk, P., Del-Favero, J., and van Broeckhoven, C. (2005). Genomic architecture of human 17q21 linked to frontotemporal dementia uncovers a highly homologous family of low-copy repeats in the tau region. *Hum. Mol. Genet.* 14, 1753–1762.
- Dafinca, R., Scaber, J., Ababneh, N., Lalic, T., Weir, G., Christian, H., Vowles, J., Douglas, A.G., Fletcher-Jones, A., Browne, C., et al. (2016). C9orf72 hexanucleotide expansions are associated with altered endoplasmic reticulum calcium homeostasis and stress granule formation in induced pluripotent stem cell-derived neurons from patients with amyotrophic lateral sclerosis and frontotemporal dementia. *Stem Cells* 34, 2063–2078.
- Delacourte, A., Robitaille, Y., Sergeant, N., Buee, L., Hof, P.R., Wattez, A., Laroche-Chollette, A., Mathieu, J., Chagnon, P., and Gauvreau, D. (1996). Specific pathological Tau protein variants characterize Pick's disease. *J. Neuropathol. Exp. Neurol.* 55, 159–168.
- Dixit, R., Ross, J.L., Goldman, Y.E., and Holzbaur, E.L. (2008). Differential regulation of dynein and kinesin motor proteins by tau. *Science* 319, 1086–1089.



- Ehrlich, M., Hallmann, A.L., Reinhardt, P., Arauzo-Bravo, M.J., Korr, S., Ropke, A., Psathaki, O.E., Ehling, P., Meuth, S.G., Oblak, A.L., et al. (2015). Distinct neurodegenerative changes in an induced pluripotent stem cell model of frontotemporal dementia linked to mutant TAU protein. *Stem Cell Reports* 5, 83–96.
- Fernandes, H.J., Hartfield, E.M., Christian, H.C., Emmanouilidou, E., Zheng, Y., Booth, H., Bogetofte, H., Lang, C., Ryan, B.J., Sardi, S.P., et al. (2016). ER stress and autophagic perturbations lead to elevated extracellular alpha-synuclein in GBA-N370S Parkinson's iPSC-derived dopamine neurons. *Stem Cell Reports* 6, 342–356.
- Goedert, M., Spillantini, M.G., Jakes, R., Rutherford, D., and Crowther, R.A. (1989). Multiple isoforms of human microtubule-associated protein tau: sequences and localization in neurofibrillary tangles of Alzheimer's disease. *Neuron* 3, 519–526.
- Hartfield, E.M., Yamasaki-Mann, M., Ribeiro Fernandes, H.J., Vowles, J., James, W.S., Cowley, S.A., and Wade-Martins, R. (2014). Physiological characterisation of human iPSC-derived dopaminergic neurons. *PLoS One* 9, e87388.
- Hayesmoore, J.B., Bray, N.J., Cross, W.C., Owen, M.J., O'Donovan, M.C., and Morris, H.R. (2009). The effect of age and the H1c MAPT haplotype on MAPT expression in human brain. *Neurobiol. Aging* 30, 1652–1656.
- Hoglinger, G.U., Melhem, N.M., Dickson, D.W., Sleiman, P.M., Wang, L.S., Klei, L., Rademakers, R., de Silva, R., Litvan, I., Riley, D.E., et al. (2011). Identification of common variants influencing risk of the tauopathy progressive supranuclear palsy. *Nat. Genet.* 43, 699–705.
- Hutton, M., Lendon, C.L., Rizzu, P., Baker, M., Froelich, S., Houlden, H., Pickering-Brown, S., Chakraverty, S., Isaacs, A., Grover, A., et al. (1998). Association of missense and 5'-splice-site mutations in tau with the inherited dementia FTDP-17. *Nature* 393, 702–705.
- Iovino, M., Agathou, S., Gonzalez-Rueda, A., Del Castillo Velasco-Herrera, M., Borroni, B., Alberici, A., Lynch, T., O'Dowd, S., Geti, I., Gaffney, D., et al. (2015). Early maturation and distinct tau pathology in induced pluripotent stem cell-derived neurons from patients with MAPT mutations. *Brain* 138, 3345–3359.
- Kar, A., Havlioglu, N., Tam, W.Y., and Wu, J.Y. (2006). RBM4 interacts with an intronic element and stimulates tau exon 10 inclusion. *J. Biol. Chem.* 281, 24479–24488.
- Kouri, N., Ross, O.A., Dombroski, B., Younkin, C.S., Serie, D.J., Soto-Ortolaza, A., Baker, M., Finch, N.C., Yoon, H., Kim, J., et al. (2015). Genome-wide association study of corticobasal degeneration identifies risk variants shared with progressive supranuclear palsy. *Nat. Commun.* 6, 7247.
- Kriks, S., Shim, J.W., Piao, J., Ganat, Y.M., Wakeman, D.R., Xie, Z., Carrillo-Reid, L., Auyeung, G., Antonacci, C., Buch, A., et al. (2011). Dopamine neurons derived from human ES cells efficiently engraft in animal models of Parkinson's disease. *Nature* 480, 547–551.
- Kwok, J.B., Teber, E.T., Loy, C., Hallupp, M., Nicholson, G., Mellick, G.D., Buchanan, D.D., Silburn, P.A., and Schofield, P.R. (2004). Tau haplotypes regulate transcription and are associated with Parkinson's disease. *Ann. Neurol.* 55, 329–334.
- Majounie, E., Cross, W., Newsday, V., Dillman, A., Vandrovцова, J., Morris, C.M., Nalls, M.A., Ferrucci, L., Owen, M.J., O'Donovan, M.C., et al. (2013). Variation in tau isoform expression in different brain regions and disease states. *Neurobiol. Aging* 34, 1922.e7–1922.e12.
- Myers, A.J., Pittman, A.M., Zhao, A.S., Rohrer, K., Kaleem, M., Marlowe, L., Lees, A., Leung, D., McKeith, I.G., Perry, R.H., et al. (2007). The MAPT H1c risk haplotype is associated with increased expression of tau and especially of 4 repeat containing transcripts. *Neurobiol. Dis.* 25, 561–570.
- Nalls, M.A., Pankratz, N., Lill, C.M., Do, C.B., Hernandez, D.G., Saad, M., DeStefano, A.L., Kara, E., Bras, J., Sharma, M., et al. (2014). Large-scale meta-analysis of genome-wide association data identifies six new risk loci for Parkinson's disease. *Nat. Genet.* 46, 989–993.
- Piva, F., Giulietti, M., Burini, A.B., and Principato, G. (2012). SpliceAid 2: a database of human splicing factors expression data and RNA target motifs. *Hum. Mutat.* 33, 81–85.
- Sandor, C., Robertson, P., Lang, C., Heger, A., Booth, H., Vowles, J., Witty, L., Bowden, R., Hu, M., Cowley, S.A., et al. (2017). Transcriptomic profiling of purified patient-derived dopamine neurons identifies convergent perturbations and therapeutics for Parkinson's disease. *Hum. Mol. Genet.* 26, 552–566.
- Sergeant, N., David, J.P., Lefranc, D., Vermersch, P., Wattez, A., and Delacourte, A. (1997). Different distribution of phosphorylated tau protein isoforms in Alzheimer's and Pick's diseases. *FEBS Lett.* 412, 578–582.
- Sherry, S.T., Ward, M.H., Kholodov, M., Baker, J., Phan, L., Smigielski, E.M., and Sirotkin, K. (2001). dbSNP: the NCBI database of genetic variation. *Nucleic Acids Res.* 29, 308–311.
- Silva, M.C., Cheng, C., Mair, W., Almeida, S., Fong, H., Biswas, M.H., Zhang, Z., Huang, Y., Temple, S., Coppola, G., et al. (2016). Human iPSC-derived neuronal model of tau-A152T frontotemporal dementia reveals tau-mediated mechanisms of neuronal vulnerability. *Stem Cell Reports* 7, 325–340.
- Spillantini, M.G., Murrell, J.R., Goedert, M., Farlow, M.R., Klug, A., and Ghetti, B. (1998). Mutation in the tau gene in familial multiple system tauopathy with presenile dementia. *Proc. Natl. Acad. Sci. USA* 95, 7737–7741.
- Sposito, T., Preza, E., Mahoney, C.J., Seto-Salvia, N., Ryan, N.S., Morris, H.R., Arber, C., Devine, M.J., Houlden, H., Warner, T.T., et al. (2015). Developmental regulation of tau splicing is disrupted in stem cell-derived neurons from frontotemporal dementia patients with the 10 + 16 splice-site mutation in MAPT. *Hum. Mol. Genet.* 24, 5260–5269.
- Tobin, J.E., Latourelle, J.C., Lew, M.F., Klein, C., Suchowersky, O., Shill, H.A., Golbe, L.I., Mark, M.H., Growdon, J.H., Wooten, G.F., et al. (2008). Haplotypes and gene expression implicate the MAPT region for Parkinson disease: the GenePD study. *Neurology* 71, 28–34.
- Trabzuni, D., Wray, S., Vandrovцова, J., Ramasamy, A., Walker, R., Smith, C., Luk, C., Gibbs, J.R., Dillman, A., Hernandez, D.G., et al. (2012). MAPT expression and splicing is differentially regulated by



brain region: relation to genotype and implication for tauopathies. *Hum. Mol. Genet.* *21*, 4094–4103.

Vossel, K.A., Xu, J.C., Fomenko, V., Miyamoto, T., Suberbielle, E., Knox, J.A., Ho, K., Kim, D.H., Yu, G.Q., and Mucke, L. (2015). Tau reduction prevents Abeta-induced axonal transport deficits by blocking activation of GSK3beta. *J. Cell Biol.* *209*, 419–433.

Wang, J., Gao, Q.S., Wang, Y., Lafyatis, R., Stamm, S., and Andreadis, A. (2004). Tau exon 10, whose missplicing causes frontotemporal dementia, is regulated by an intricate interplay of *cis* elements and *trans* factors. *J. Neurochem.* *88*, 1078–1090.

Williams, D.R. (2006). Tauopathies: classification and clinical update on neurodegenerative diseases associated with microtubule-associated protein tau. *Intern. Med. J.* *36*, 652–660.